NASA TM X-507

TECHNICAL MEMORANDUM

X-507

FREE-FLIGHT MEASUREMENTS OF DRAG AND STATIC STABILITY FOR A BLUNT-NOSED 10° HALF-ANGLE CONE AT MACH NUMBER 15

By Dale L. Compton

Ames Research Center
Moffett Field, Calif.

NATIONAL AERONAUTICS AND SPACE ADMINISTRATION

WASHINGTON April 1961

NATIONAL AERONAUTICS AND SPACE ADMINISTRATION

TECHNICAL MEMORANDUM X-507

FREE-FLIGHT MEASUREMENTS OF DRAG AND STATIC STABILITY FOR A BLUNT-NOSED 10° HALF-ANGLE CONE AT MACH NUMBER 15*

By Dale L. Compton

SUMMARY

Experimental free-flight measurements of drag and static stability have been made on a blunt-nosed 10° half-angle cone at a nominal Mach number of 15 and a nominal Reynolds number of 2.8×10^6. It was found that the model is statically stable throughout the angle-of-attack range tested, and that the experimental pitching moment could be approximated by a cubic polynomial.

The results are compared with two simple theories. Both theories show good agreement with the experimental drag coefficient but overestimate, by approximately 50 percent, the slope of the experimental moment curve at zero angle of attack.

INTRODUCTION

At the present time, little experimental data is available at hypersonic Mach numbers on the stability of blunt, nonlifting shapes suitable for atmosphere re-entry. The purpose of this report is to present data at a nominal Mach number of 15 and a nominal Reynolds number of 2.8×10^6 on the static stability and drag of a blunt-nosed 10° half-angle cone, and to compare the results with two simple theories.

SYMBOLS

A	frontal area, sq ft
C_{L_α}	lift-curve slope, per radian
C_D	drag coefficient, $\frac{\text{drag}}{q_\infty A}$, dimensionless
C_m	pitching-moment coefficient, $\frac{\text{pitching moment}}{q_\infty A d}$, dimensionless

*Title, Unclassified

C_{m_α}	pitching-moment-curve slope, per radian
C_{N_α}	normal-force-curve slope, per radian
C_p	pressure coefficient
d	maximum body diameter, ft
I_y	transverse moment of inertia, slug-ft^2
m	mass of model, slugs
M	Mach number, dimensionless
M_o	$\frac{\rho A d}{2I_y} C_m$, ft^{-2}
$M_{1,2}$	cubic restoring moment coefficients, defined by equation (3), ft^{-2}
q_∞	free-stream dynamic pressure, lb/sq ft
R	Reynolds number based on maximum diameter, dimensionless
V	velocity along flight path, ft/sec
X	distance along flight path, ft
x_{cg}	axial distance from model nose to center-of-gravity position, ft
x_{cp}	axial distance from model nose to center-of-pressure position, ft
α	angle of pitch (in the vertical plane), deg
α_R	$\sqrt{\alpha^2 + \beta^2}$, deg
$\overline{\alpha}_R$	root mean square resultant angle of attack defined in equation (2), deg
β	angle of yaw (in the horizontal plane), deg
λ	wave length of pitching oscillation, ft/cycle
θ	slope of the body meridian
ρ	free-stream air density, slugs/cu ft
ξ	dummy variable in equation (2)

Subscripts

max	maximum
min	minimum
s	stagnation point

MODELS AND TESTS

Figure 1 is a drawing of the model. It has a maximum diameter of 0.45 inch and a center-of-gravity position at 48.3 percent of the diameter from the nose. The front section was machined from titanium and the rear section from 7075-T6 aluminum in order to obtain the desired center-of-gravity location. The small screw on the rear was used to hold the model flush on the front face of the sabot. The point on the base of the screw served as a reference point for reading the position of the model in the shadowgraphs.

A picture of a model in its sabot is shown in figure 2. (The apparent roughness on the model is caused by wax which was sprayed on in order to reduce highlights in the photograph.) The sabot was machined from ethyl cellulose plastic and was split in half to allow model and sabot separation which was accomplished by the action of aerodynamic forces on the front lip of the sabot.

All tests were conducted by firing models into the Mach number 3 countercurrent air stream of the Ames Supersonic Free-Flight Wind Tunnel. The models were launched from a shock-heated helium gun with a 90-mm diameter pump tube and a 37-mm diameter smooth-bore launch tube. The nominal velocity of the model was 8500 feet per second, which resulted in a nominal Mach number of 15 and a nominal Reynolds number of 2.8×10^6. Nine data stations, spaced at 3-foot intervals along the length of the wind tunnel, recorded model positions on shadowgraphs. Two typical shadowgraphs are shown in figure 3. Time intervals between stations were recorded on chronographs. The wind tunnel and its instrumentation are described more fully in reference 1.

The data from each run were a time-distance history and an angle of pitch and yaw history obtained from the shadowgraphs and from the chronograph readings. The drag coefficient was computed from the time-distance history by the method described in reference 2. The wave length of each motion was determined from the angle of pitch and yaw history, and the static stability derivative, C_{m_α}, was computed from the equation (ref. 3)

$$C_{m_\alpha} = - \frac{8\pi^2 I_y}{\lambda^2 \rho A d} \qquad (1)$$

A linear variation of pitching moment with angle of attack is assumed in the development of equation (1).

THEORETICAL PREDICTIONS

Theoretical values for the drag and static stability were computed from two methods. The first was the familiar modified Newtonian impact theory, where $C_p = C_{p_s} \sin^2\theta$. Computations for this method were carried only to the angle of attack at which part of the body becomes rearward facing, $\alpha = 10^\circ$. The second method will be referred to as the modified Newtonian Prandtl-Meyer method and consisted of matching the modified Newtonian pressure coefficient with a Prandtl-Meyer expansion at the point on the body where the pressure gradients given by both methods were the same (see ref. 4). When the body was at angle of attack, the pressures on the body in the plane of pitch were assumed to have the modified Newtonian Prandtl-Meyer value for the local angle presented to the flow, and a cosine variation of pressure was assumed around the body between the upper and lower meridians. No computational difficulty existed for carrying this method beyond $\alpha = 10^\circ$ and the computations were carried to $\alpha = 20^\circ$.

RESULTS AND DISCUSSION

Experimental measurements of drag and static stability are presented in table I. Included in this table are the Mach numbers, Reynolds numbers, maximum and minimum resultant angles of attack (the largest and smallest combined angles of pitch and yaw), and pertinent model measurements for each flight.

The experimental drag data are shown in figure 4, where C_D is plotted as a function of root mean square resultant angle of attack, $\bar{\alpha}_R$, defined as

$$\bar{\alpha}_R^2 = \frac{\int_0^X (\alpha^2 + \beta^2)\,d\xi}{\int_0^X d\xi} \qquad (2)$$

(It is shown in ref. 5 that $\bar{\alpha}_R$ is the correct parameter against which to plot C_D for free-flight tests.) Theoretical values of the drag coefficient computed by the two methods previously described are also shown in figure 4. (No allowance has been made for base drag since computations indicate that it will be less than 1 percent of the calculated values.) It can be seen that both theories predict drag coefficients about 10 percent greater than the experimental values.

The raw experimental static stability data are shown in figure 5, where the values of C_{m_α}, computed by assuming a linear variation of

pitching moment with angle of attack, are plotted as a function of maximum resultant angle of attack. The vertical bar at each point shows the possible scatter due to experimental error. Thus the observed variation in C_{m_α} with angle of attack must be due to a nonlinearity in the pitching-moment curve. The group of data was then fitted by the method of Rasmussen (ref. 6). In this method a pitching moment is assumed of the form

$$M_O = - M_1\left(\frac{\alpha_R}{57.3}\right) - 2M_2\left(\frac{\alpha_R}{57.3}\right)^3 \tag{3}$$

where

$$M_O = \frac{\rho A d}{2I_y} C_m \tag{4}$$

and a simple relation is derived between the C_{m_α} obtained from free-flight data fitted by linear equations and the true local value of the pitching moment. (The true local value is that which would be observed in a wind tunnel with the model held at constant angle of attack.) The pitching-moment coefficients, M_1 and M_2, were computed from the observed wave lengths and maximum and minimum resultant pitching amplitudes by the equation (derived in ref. 6)

$$\left(\frac{2\pi}{\lambda}\right)^2 = M_1 + 1.44M_2\left[\left(\frac{\alpha_{R_{max}}}{57.3}\right)^2 + \left(\frac{\alpha_{R_{min}}}{57.3}\right)^2\right] \tag{5}$$

Since this method requires only two runs to determine M_1 and M_2, the data were fitted by the method of least squares, and the coefficients were found to be

$$M_1 = 0.0572$$

$$M_2 = 0.149$$

An indication of the validity of the assumption of a cubic pitching moment may be seen in figure 6, where $(2\pi/\lambda)^2$ is plotted as a function of $(\alpha_{R_{max}}/57.3)^2 + (\alpha_{R_{min}}/57.3)^2$. It can be seen from the plot that the three points fall very closely on a straight line and therefore the cubic pitching moment is an excellent assumption.

From the coefficients, the true local values of C_{m_α} and C_m were computed and are shown plotted as a function of angle of attack in figures 7 and 8, respectively. The values of C_{m_α}, obtained from the linear analysis of the raw data, are shown in figure 7 as bars over the angle-of-attack range covered by each flight.

The values of C_{m_α} and C_m, computed from modified Newtonian theory and modified Newtonian Prandtl-Meyer theory, are also shown in figures 7 and 8. Both theories predict values of C_{m_α} about 50 percent greater than measured at $\alpha = 0^\circ$. It should be pointed out that while this

discrepancy appears serious, its magnitude is dependent on the proximity of the center of gravity to the center of pressure, and a better indication of the ability of the theory to successfully predict stability is its ability to predict center of pressure. Both theories indicate a center of pressure at 53.8 percent of the diameter from the nose, indicating a theoretical static margin of 5.5 percent of the diameter. It was not possible to obtain experimental center-of-pressure measurements from the test data, but an estimate based on the experimental C_{m_α} and the modified Newtonian value for C_{N_α} places x_{cp} at 51.3 percent, indicating the experimental static margin to be 3.0 percent. Hence the discrepancy between the theoretical center of pressure and the estimated actual center of pressure is on the order of 3 percent of the diameter.

The agreement between modified Newtonian Prandtl-Meyer theory and experiment improves in this case with increasing angle of attack, the difference being only 5 percent in C_{m_α} and 18 percent in C_m at $\alpha = 20^\circ$.

CONCLUSIONS

Experimental free-flight measurements of drag and static stability have been made on a blunt-nosed 10° half-angle cone at a nominal Mach number of 15 and a nominal Reynolds number of 2.8×10^6.

The configuration was found to be statically stable throughout the angle-of-attack range tested. It was found that the experimental data could be correlated very well with the assumption of a cubic pitching-moment curve.

Two simple theories - modified Newtonian and modified Newtonian with a Prandtl-Meyer expansion matched at the point on the surface where the pressure gradients are equal - were found to overestimate the slope of the moment curve at $\alpha = 0^\circ$ by approximately 50 percent.

Both theories gave a satisfactory estimate of the drag coefficient.

Ames Research Center
National Aeronautics and Space Administration
Moffett Field, Calif., Oct. 17, 1960

REFERENCES

1. Seiff, Alvin: A Free-Flight Wind Tunnel for Aerodynamic Testing at Hypersonic Speeds. NACA Rep. 1222, 1955.

2. Seiff, Alvin: A New Method for Computing Drag Coefficients From Ballistic Range Data. Jour. Aero. Sci., vol. 25, no. 2, Feb. 1958, pp. 133-134.

3. Seiff, Alvin, Sommer, Simon C., and Canning, Thomas N.: Some Experiments at High Supersonic Speeds on the Aerodynamic and Boundary-Layer Transition Characteristics of High Drag Bodies of Revolution. NACA RM A56I05, 1957.

4. Lees, Lester, and Kubota, Toshi: Inviscid Hypersonic Flow Over Blunt-Nosed Slender Bodies. Jour. Aero. Sci., vol. 24, no. 3, March 1957, pp. 195-202.

5. Seiff, Alvin, and Wilkins, Max E.: Experimental Investigation of a Hypersonic Glider Configuration at a Mach Number of 6 and at Full-Scale Reynolds Numbers. NASA TN D-341, 1960.

6. Rasmussen, Maurice L.: Determination of Nonlinear Pitching-Moment Characteristics of Axially Symmetric Models From Free-Flight Data. NASA TN D-144, 1960.

TABLE I.- TEST CONDITIONS AND DATA

Test number	M	$R \times 10^{-6}$	$\alpha_{R_{max}}$, deg	$\alpha_{R_{min}}$, deg	$\bar{\alpha}_R$, deg	C_D	C_{m_α} (linear analysis)	d, in.	$I_y \times 10^8$ slug-ft^2	$\frac{x_{cg}}{d}$
592	14.59	3.39	26.5	1.7	18.5	0.747	-0.067	0.4499	1.87	0.482
660	16.46	2.55	33.0	9.5	25.1	.798	-.087	.4503	1.87	.484
661	15.75	2.46	16.5	5.8	12.0	.730	-.050	.4495	1.92	.483

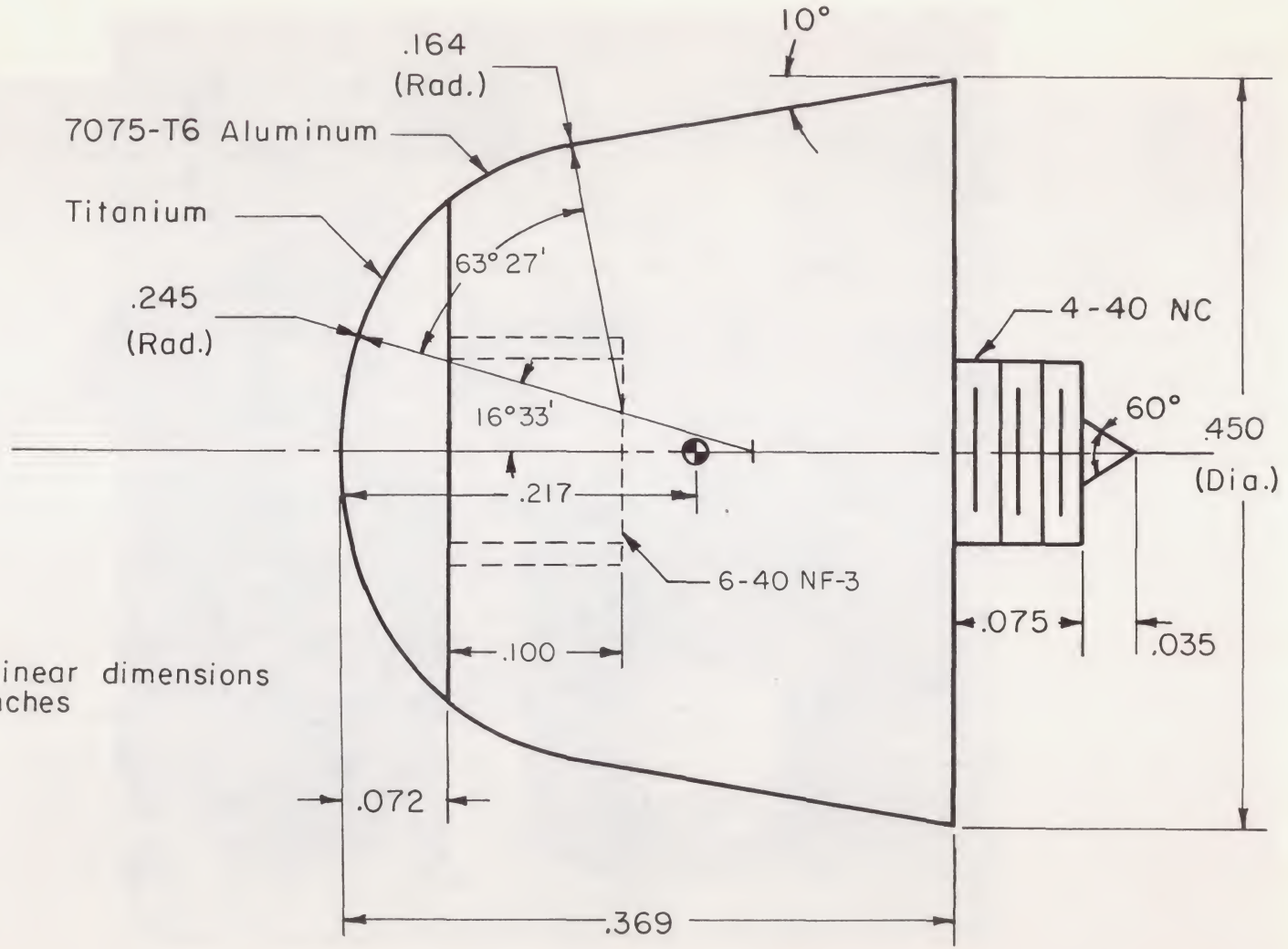

Figure 1.- Sketch of model

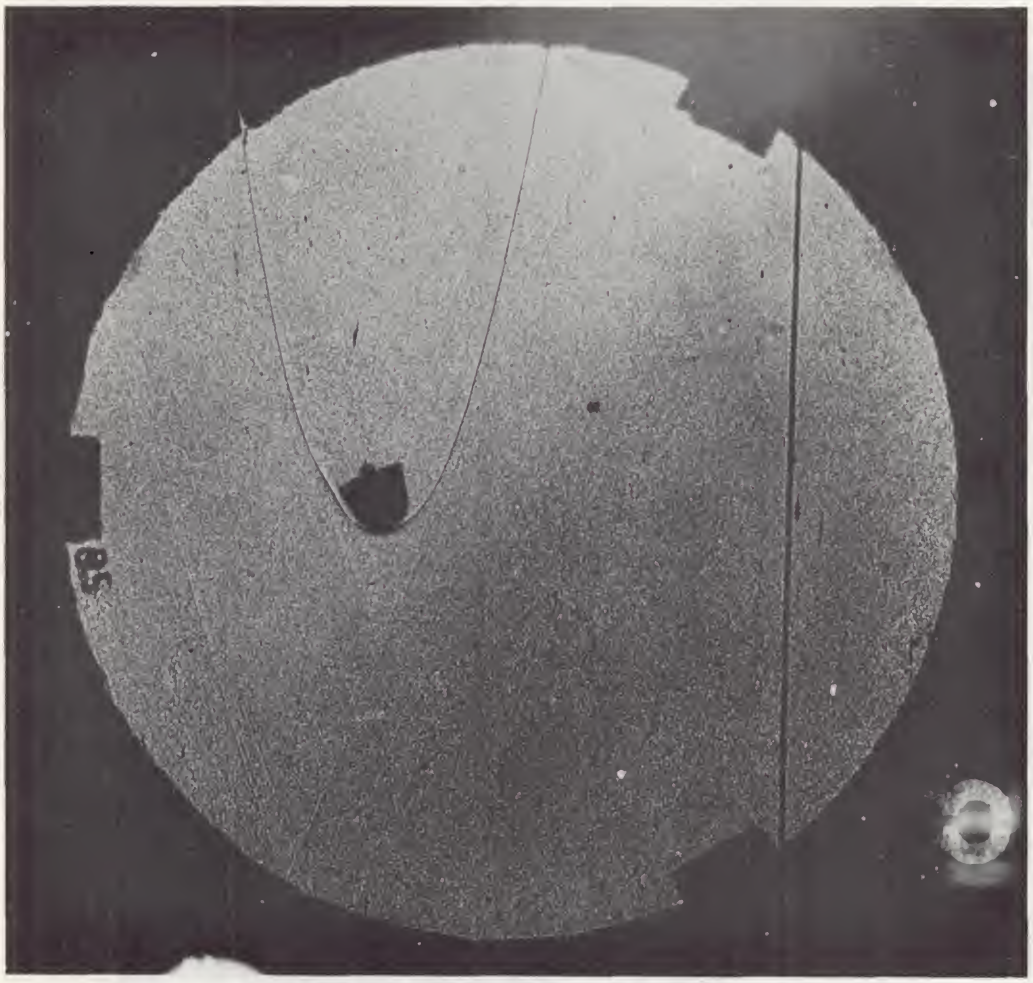

A-25809

(b) M = 13.9, R = 3.24×10^6, $\alpha = 22.8^\circ$

Figure 3.- Concluded.

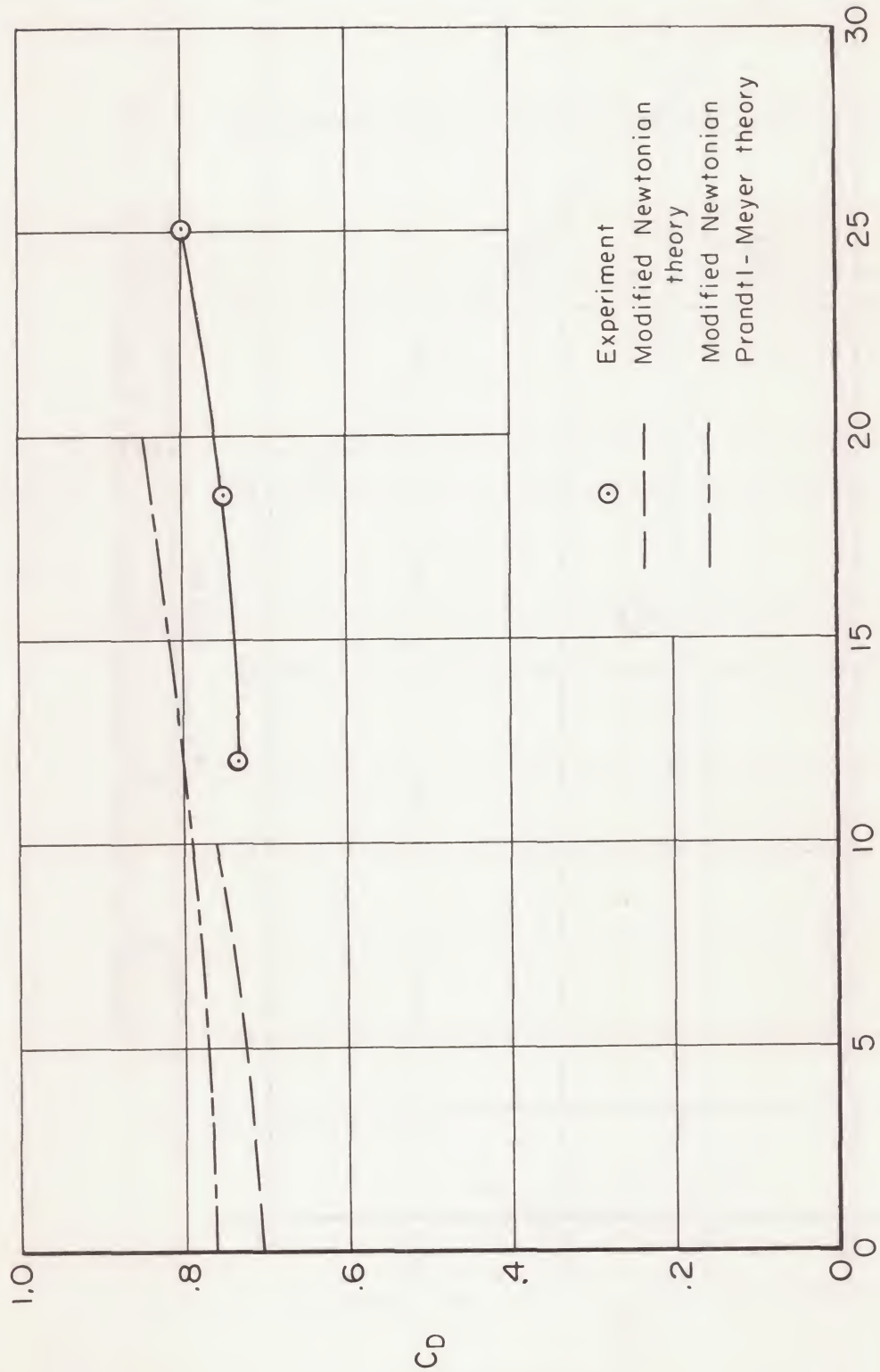

Figure 4.- Drag results.

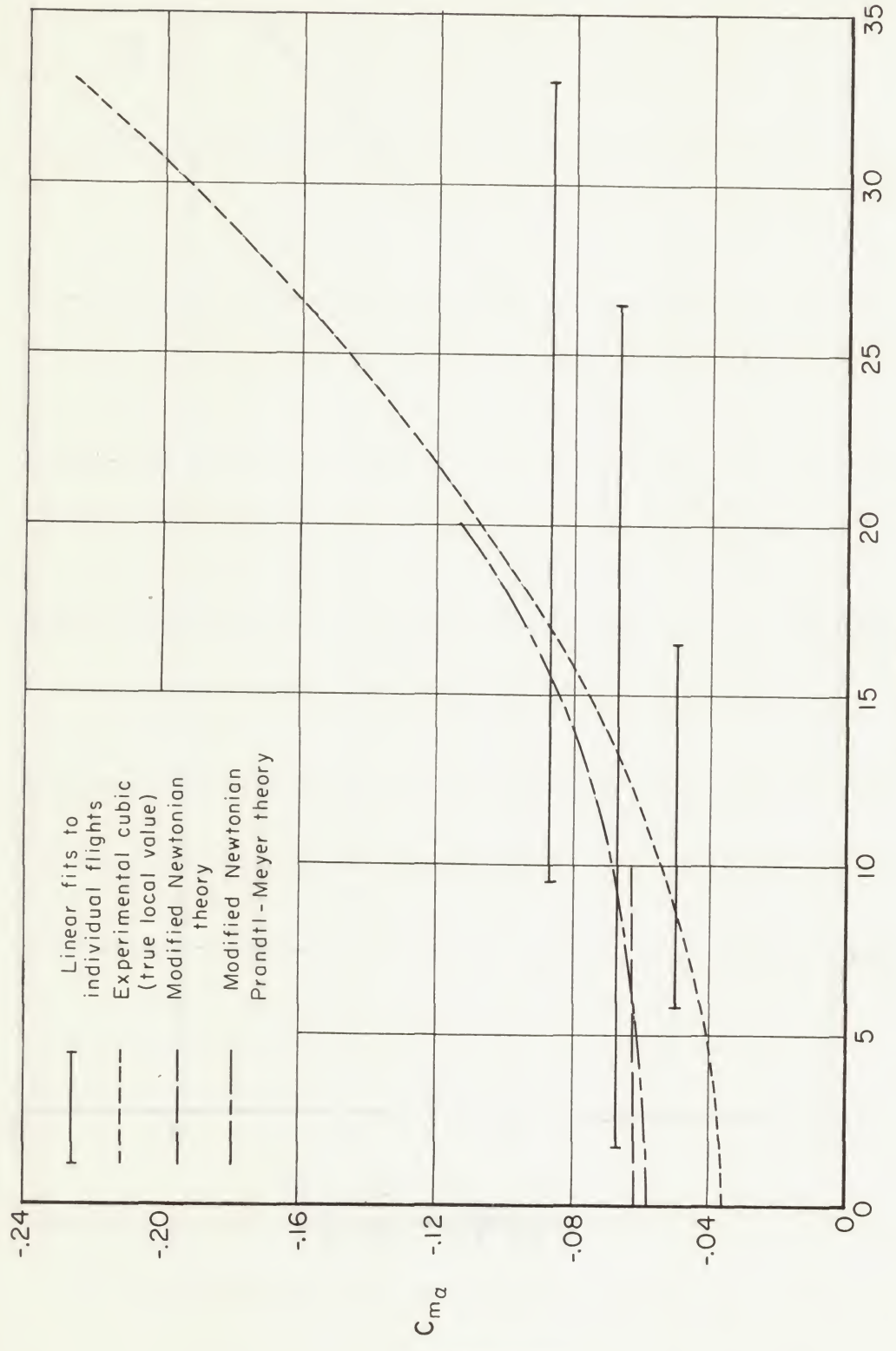

Figure 7.- Static stability results.

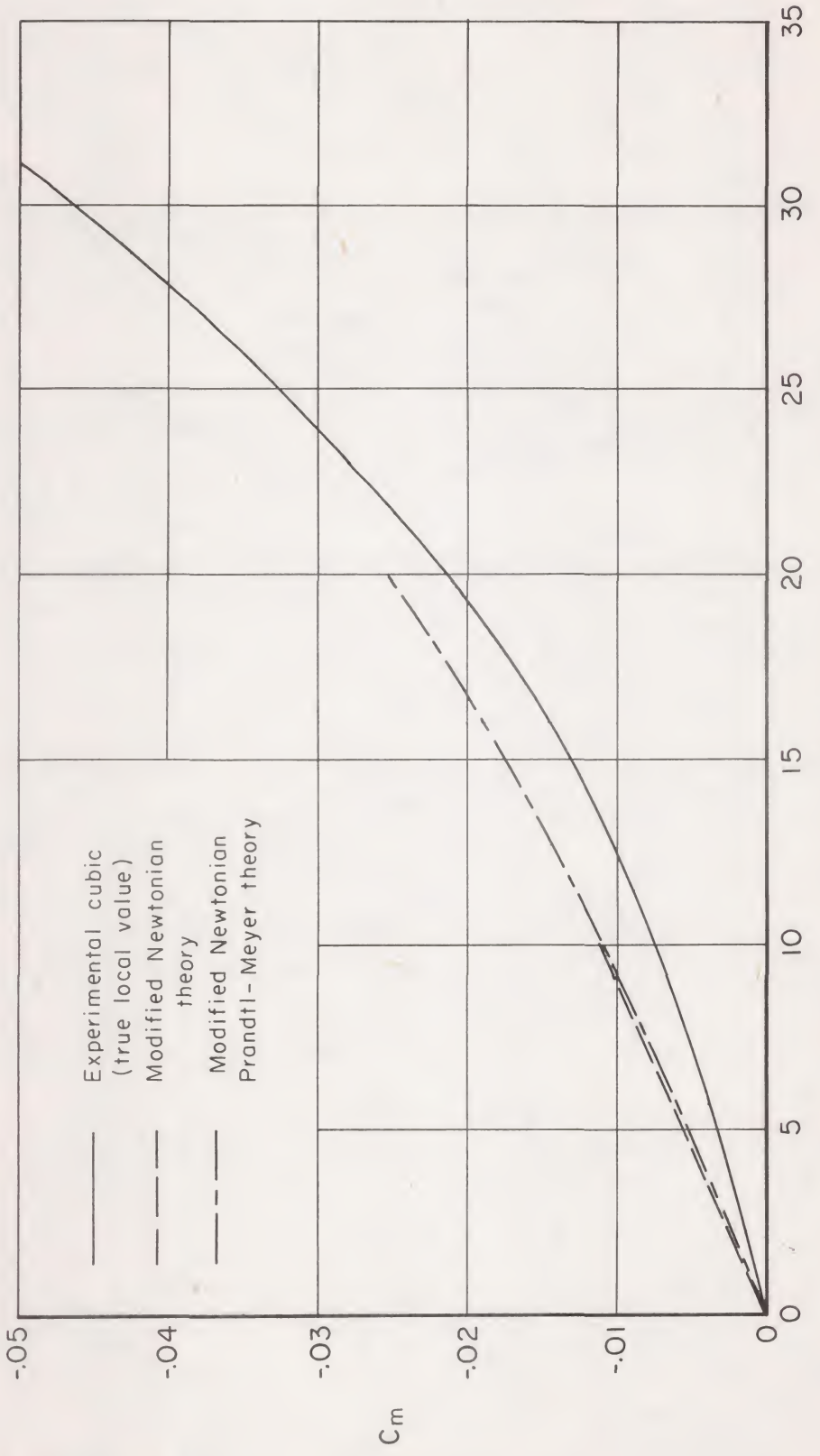

Figure 8.- Pitching-moment curve.